Intercomparison of Rain Gauge, Radar, and Satellite-Based Precipitation Estimates with Emphasis on Hydrologic Forecasting

KORAY K. YILMAZ

Department of Hydrology and Water Resources, The University of Arizona, Tucson, Arizona

TERRI S. HOGUE

Department of Civil and Environmental Engineering, University of California, Los Angeles, Los Angeles, California

KUO-LIN HSU AND SOROOSH SOROOSHIAN

Department of Civil and Environmental Engineering, University of California, Irvine, Irvine, California

HOSHIN V. GUPTA

Department of Hydrology and Water Resources, The University of Arizona, Tucson, Arizona

THORSTEN WAGENER

Department of Civil and Environmental Engineering, The Pennsylvania State University, University Park, Pennsylvania

(Manuscript received 14 October 2004, in final form 7 February 2005)

ABSTRACT

This study compares mean areal precipitation (MAP) estimates derived from three sources: an operational rain gauge network (MAPG), a radar/gauge multisensor product (MAPX), and the Precipitation Estimation from Remotely Sensed Information using Artificial Neural Networks (PERSIANN) satellite-based system (MAPS) for the time period from March 2000 to November 2003. The study area includes seven operational basins of varying size and location in the southeastern United States. The analysis indicates that agreements between the datasets vary considerably from basin to basin and also temporally within the basins. The analysis also includes evaluation of MAPS in comparison with MAPG for use in flow forecasting with a lumped hydrologic model [Sacramento Soil Moisture Accounting Model (SAC-SMA)]. The latter evaluation investigates two different parameter sets, the first obtained using manual calibration on historical MAPG, and the second obtained using automatic calibration on both MAPS and MAPG, but over a shorter time period (23 months). Results indicate that the overall performance of the model simulations using MAPS depends on both the bias in the precipitation estimates and the size of the basins, with poorer performance in basins of smaller size (large bias between MAPG and MAPS) and better performance in larger basins (less bias between MAPG and MAPS). When using MAPS, calibration of the parameters significantly improved the model performance.

1. Introduction

Many hydrologic simulation studies, whether related to climate change scenarios, flood forecasting, or water management, depend heavily on the availability of good-quality precipitation estimates. Difficulties in estimating precipitation arise in many remote parts of the world and particularly in developing countries where ground-based measurement networks (rain gauges or weather radar) are either sparse or nonexistent, mainly due to the high costs of establishing and maintaining infrastructure. This situation imposes an important limitation on the possibility and reliability of hydrologic forecasting and early warning systems in these regions. For example, recent monsoon flooding (June–July

Corresponding author address: Koray K. Yilmaz, Department of Hydrology and Water Resources, The University of Arizona, Tucson, AZ 85721-0011.
E-mail: koray@hwr.arizona.edu

2004) in Bangladesh caused massive damage to the land, infrastructure, and economy and affected more than 23 million people.

The International Association of Hydrological Sciences (IAHS) recently launched an initiative called the Decade on Predictions in Ungauged Basins (PUB), aimed at achieving major advances in the capacity to make reliable predictions in "ungauged" basins (Sivapalan et al. 2003). Ungauged is used to indicate locations where measurements of the variables of interest are either too few or too poor in quality, or not available at all. In particular, where measurements of the system response (e.g., streamflow) are lacking, prior estimates of the model parameters cannot be improved via calibration (Gupta et al. 2005). However, where measurements of the system input (e.g., precipitation) are missing, the model cannot even be driven to provide forecasts.

Recent improvements in the ability of satellite-based precipitation retrieval algorithms to produce estimates (with global coverage) at high space and time resolutions makes them potentially attractive for hydrologic forecasting in ungauged basins. This study provides a test of the Precipitation Estimation from Remotely Sensed Information using Artificial Neural Networks (PERSIANN; see section 3d for description) satellite-based product using several basins in the southeastern United States where other sources of precipitation estimates (rain gauge, weather radar) exist for comparison. The National Weather Service (NWS) is the agency responsible for providing river forecasts for the United States. For this purpose, the NWS routinely uses mean areal precipitation estimates from rain gauge networks and recently from radar/gauge multisensor products to drive the Sacramento Soil Moisture Accounting Model (SAC-SMA; Burnash et al. 1973; Burnash 1995). Hereafter, MAPG, MAPX, and MAPS will denote basin mean areal precipitation (MAP) estimates derived from the rain gauge network, the Weather Surveillance Radar-1998 Doppler (WSR-88D) multisensor product, and the PERSIANN satellite-based system, respectively.

The research questions addressed in this study are as follows.

1) How do precipitation estimates based on the rain gauge network, radar/gauge multisensor product, and satellite-based algorithm compare at the space–time scale currently utilized by the NWS for operational hydrologic forecasting procedures within the selected study basins (basin MAP at 6-h intervals)?
2) How does the performance of a hydrologic model change when the rain gauge–based precipitation estimates are replaced by satellite-based estimates? In other words, how do differences between precipitation estimates affect the resulting simulated flow forecasts?

The importance of the second question is twofold. If the model adequately captures the dynamics of water distribution and movement in the basin and the calibration is robust, a comparison of the simulated and observed flow will serve as an independent check on the accuracy of the precipitation estimates. Further, because the rainfall-runoff transformation acts as a low-pass filter, it is interesting to determine whether the bias error in the precipitation estimates becomes attenuated, thereby helping to clarify what level of input accuracy is required for hydrological prediction (Andreassian et al. 2001).

The paper is organized as follows. Relevant background information is presented in section 2. Details of the study area, datasets, and the hydrologic model are given in section 3. Methods and calibration procedure are presented in section 4. The results are summarized in section 5, and conclusions and recommendations are offered in section 6.

2. Background

Whether measured directly by rain gauges or indirectly by remote sensing techniques, all precipitation estimates contain uncertainty. While rain gauges provide a direct measurement of precipitation reaching the ground, they may contain significant bias arising from coarse spatial resolution (yielding underestimation especially during events with low spatial coherency, i.e., convective showers), location, wind, and mechanical errors among others (Groisman and Legates 1994). According to Legates and DeLiberty (1993) rain gauges may underestimate the true precipitation by about 5%. Radar estimates hold promise for hydrologic studies by providing data at high spatial and temporal resolution over extended areas but suffer from bias due to several factors including hardware calibration, uncertain Z–R relationships (Winchell et al. 1998; Morin et al. 2003), ground clutter, brightband contamination, mountain blockage, anomalous propagation, and range-dependent bias (Smith et al. 1996). Recent advances in satellite-based remote sensing have enabled scientists to develop precipitation estimates having near-global coverage, thereby providing data for regions where ground-based networks are sparse or unavailable (Sorooshian et al. 2000). However, this advantage is offset by the indirect nature of the satellite observables (e.g., cloud-top reflectance or thermal radiance) as measures

of surface precipitation intensity (Petty and Krajewski 1996).

In general, satellite-based precipitation estimation algorithms use information from two primary sources. The infrared (IR) channels from geosynchronous satellites are used to establish a relationship between cloud-top conditions and rainfall rate at the base of the cloud. This relationship can be developed at relatively high spatial (~4 km × 4 km) and temporal (30 min) resolution. The microwave (MW) channels from low-orbiting satellites are used to more directly infer precipitation rates by penetrating the cloud, but a low-orbiting satellite can retrieve only one or two samples per day. The relative strengths and weaknesses of various sources have been exploited in the development of algorithms that combine and make the best use of each source. The NWS uses a multivariate objective analysis scheme to merge radar and rain gauge estimates (Fulton et al. 1998). In the case of satellite-based estimates, algorithms have been designed that merge satellite imagery with other kinds of satellite imagery (Sorooshian et al. 2000; Kuligowski 2002), numerical weather prediction (NWP) models (Grimes and Diop 2003), rain gauges (Adler et al. 2000; Huffman et al. 2001), and rain gauges and NWP models (Xie and Arkin 1997).

Numerous studies have compared precipitation estimates from different sensors to validate the algorithms with a view to improve the quality of estimates. For example, intercomparison studies focusing on radar-based estimates include Johnson et al. (1999), Young et al. (2000), Stellman et al. (2001), and Grassotti et al. (2003). Studies focusing on satellite-based estimates include Adler et al. (2001), Krajewski et al. (2000), Rozumalski (2000), and McCollum et al. (2002). We build on this previous work by comparing all three types of precipitation estimates and take the evaluation further by examining the adequacy of satellite products for use in basinscale hydrologic modeling.

Previous radar-based precipitation intercomparison studies in the Southern Great Plains have reported that hourly digital precipitation (HDP) radar estimates (Smith et al. 1996) and radar/gauge merged stage III estimates (Johnson et al. 1999; Young et al. 2000) tend to underestimate the rain gauge estimates. Smith et al. (1996) showed that HDP estimates suffer from range-dependent underestimation bias varying between 14% and 100% depending on the season. Young et al. (2000) also observed range-dependent bias in the stage III estimates, but less than that in the HDP estimates. Smith et al. (1996) further reported that more than 30% systematic difference between precipitation estimates from adjacent radars may be present because of radar calibration differences. Grassotti et al. (2003) reported a seasonal bias between radar-only estimates developed by the Weather Service International Corporation (WSI) and rain gauges; the bias took the form of underestimation during the cold season and overestimation during the warm season. Over the Culloden Basin in Georgia, Stellman et al. (2001) found that MAPX was similar to MAPG during summer but suffered from underestimation (~50%) during the cold season.

In a study to quantify the error variance of the monthly Global Precipitation Climatology Project (GPCP) satellite-based estimates, Krajewski et al. (2000) noted significant geographical and seasonal variability in the error statistics. Their Oklahoma site showed a positive bias during the summer and a negative bias during the winter while the Georgia site showed a negative bias in the summer and winter. In a validation study over the United States, McCollum et al. (2002) found that an algorithm using microwave channels of the satellites overestimates precipitation in summer and underestimates in winter, with an east-to-west bias gradient. Rozumalski (2000) evaluated the IR-based AutoEstimator (A-E) algorithm over the Arkansas–Red Basin and reported that the A-E skill diminished when moving from warm to cold season and that 24-h A-E totals overestimated stage III precipitation by a factor of 2 during the warm season and underestimated by a factor of 0.61 during the cold season.

The effect of different precipitation scenarios on hydrologic model parameters and simulated hydrographs has been studied by various researchers (Finnerty et al. 1997; Winchell et al. 1998; Koren et al. 1999; Johnson et al. 1999; Andreassian et al. 2001; Grimes and Diop 2003; Tsintikidis et al. 1999). Among others, Grimes and Diop (2003) investigated the use of the Meteosat thermal IR imagery–based satellite precipitation estimation algorithm for flow forecasting and indicated that the inclusion of NWP model output improved the quality of modeled hydrographs. In a feasibility analysis to estimate mean areal precipitation based on visible and IR Meteosat imagery, Tsintikidis et al. (1999) indicated that semidistributed hydrologic model parameters should be recalibrated with satellite-based precipitation using spatially variable parameter values. The study of Finnerty et al. (1997) showed that SAC-SMA model parameters derived at a particular space and time scale cannot be applied at different scales without introducing significant runoff bias.

A general conclusion from the above studies is that the accuracy of both radar and satellite-based precipitation estimates depends on the calibration procedure used, the season, and the geographic location, and that the differences in these estimates can affect hydrologic predictions. This study therefore seeks to gain insight

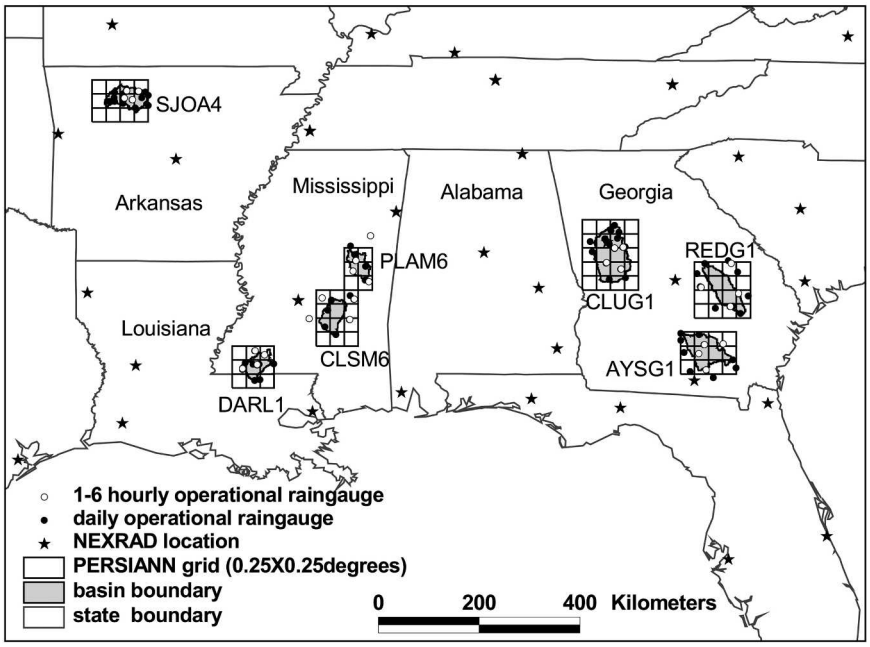

FIG. 1. Location map of the study area.

into the utility of the satellite-based estimates for hydrologic forecasting by analyzing the differences between MAPG, MAPX, and MAPS and by exploration of the corresponding performance of a hydrologic model.

3. Study area, datasets, and hydrologic model

a. Study area

The study area includes seven NWS operational basins of varying size and geographic location within the relatively humid southeastern United States (Fig. 1; Table 1). The area is free of snow and the radar beams are not blocked by mountains. The basins AYSG1, CLUG1, and REDG1 lie within the responsibility of the NWS's Southeast River Forecast Center (SERFC), and the basins CLSM6, DARL1, PLAM6, and SJOA4 lie within the responsibility of the NWS's Lower Mississippi River Forecast Center (LMRFC).

b. Rain gauge data

The RFCs use an operational rain gauge network and the National Weather Service River Forecast System (NWSRFS) to derive MAPG. We obtained the operational MAPG from RFC archives because they have already been subject to quality control procedures (and also because not all rain gauges used in the operational network are reported to other agencies). In an operational basin, 6-h MAPG is calculated as follows: (i) precipitation values obtained from operational network are accumulated to derive daily totals for each rain gauge, (ii) missing data are estimated by a distance weighting procedure, (iii) daily MAPG is computed using the Theissen polygon method and distributed to 6-h

TABLE 1. Study basin characteristics and relevant information; P is annual precipitation (rain gauges) and Q is flow.

Basin ID	Basin name	Elev (m)	Area (km^2)	P* (mm yr^{-1})	Q* (mm yr^{-1})
PLAM6	Pearl River near Burnside, MS	114.7	1346	1636.0	568.5
DARL1	Amite River near Darlington, LA	44.4	1502	1343.5	439.4
CLSM6	Leaf River near Collins, MS	60.2	1954	1660.9	562.1
SJOA4	Buffalo River near St. Joe, AR	170.8	2147	1085.0	460.5
REDG1	Ohoopee River near Reidsville, GA	22.5	2939	1171.5	271.1
AYSG1	Satilla River near Waycross, GA	20.2	3281	1243.0	243.6
CLUG1	Flint River near Culloden, GA	102.0	4774	1335.5	374.5

* Based on water years 2002–03.

values based on the 1- or 6-h rain gauges closest to the centroid of the basin in each of four quadrants (Johnson et al. 1999). Unfortunately, MAPG is unavailable for the period from May 2001 to September 2001 for the SERFC basins.

c. Radar data

The RFCs calculate operational MAPX using a multisensor product derived by merging the operational hourly rain gauge and radar (WSR-88D) precipitation estimates. The early version of the merging algorithm, known as stage II, is the result of a multivariate optimal estimation procedure (Seo et al. 1997). The mosaic of stage II product over each RFC is quality controlled by RFC personnel and termed as stage III (Fulton et al. 1998). Operational experience with the stage II/III algorithms led to development of the Multisensor Precipitation Estimator (MPE) to mitigate some of the radar deficiencies such as range degradation and beam blockage. The main objective of the MPE product is to reduce both spatially mean and local bias errors in radar-derived precipitation using rain gauges and satellite so that the final multisensor product is better than any single sensor alone (Fulton 2002). The RFCs have initiated the switch from stage II/III to the MPE algorithm. SERFC and LMRFC have switched from the stage III algorithm to the MPE algorithm in October 2002 and in October 2003, respectively. Radar/gauge multisensor products are mapped on a polar stereographic projection called the Hydrologic Rainfall Analysis Project (HRAP) grid (~4 km $\times$ 4 km). The RFCs compute MAPX by averaging the precipitation values from each HRAP bin contained in the basin (Stellman et al. 2001). We obtained the operational MAPX values from the LMRFC. Missing data for the LMRFC and all the data for the SERFC were calculated by downloading the hourly radar/gauge multisensor product from the National Oceanic and Atmospheric Administration (NOAA) Hydrologic Data Systems Group Web site (http://dipper.nws.noaa.gov/hdsb/data/nexrad/nexrad_data.html) and following the procedures listed on the NWS Hydrology Laboratory Web site (http://www.nws.noaa.gov/oh/hrl/dmip/nexrad.html). For the SERFC basins, MAPX is unavailable for August 2000 and April 2001.

d. Satellite data

The PERSIANN system (Hsu et al. 1997, 1999, 2002; Sorooshian et al. 2000) uses an artificial neural network to estimate 30-min rainfall rates at 0.25° $\times$ 0.25° spatial resolution using IR images from geosynchronous satellites [Geostationary Operational Environmental Satellite (GOES), Geostationary Meteorological Satellite (GMS), and Meteosat] and a previously calibrated neural network mapping function. The system classifies satellite images according to cloud-top IR brightness temperature and texture at and around the estimation pixel. For each class, a multivariate linear mapping function is used to relate the input features to the output rain rate. Whenever an MW-based rainfall measurement (Ferraro and Marks 1995; Kummerow et al. 1998; Weng et al. 2003) from a low-orbiting satellite [Tropical Rainfall Measuring Mission (TRMM); *NOAA-15*, *-16*, *-17*; Defense Meteorological Satellite Program (DMSP) *F-13*, *-14*, *-15*] is available, the error in each pixel is used to adjust the parameters of the associated mapping function. MAPS values are calculated by area weighting each PERSIANN grid over the basin. The PERSIANN dataset starts in March 2000. Because of an algorithm failure reported by the developers of the PERSIANN system, we removed the period from 29 January through 15 February 2003 from precipitation comparison and model simulation analysis.

e. Hydrologic model

The SAC-SMA (Burnash et al. 1973; Burnash 1995) is a lumped, conceptual rainfall-runoff model composed of a thin upper layer representing the surface soil regimes and the interception storage, and a thicker lower layer representing the deeper soil layers containing the majority of the soil moisture and groundwater storage (Brazil and Hudlow 1981). Percolation from the upper to the lower layer is controlled by a nonlinear process dependent on the contents of upper-zone free water and the deficiencies in the lower-zone storages. The model utilizes six soil moisture states and 16 parameters to describe the flow of water through the basin. The SAC-SMA model inputs are 6-h MAP and daily mean areal potential evaporation (MAPE), and output is the daily runoff. Output from the SAC-SMA is then routed through a unit hydrograph (obtained from the RFCs) to obtain streamflow values. MAPE values are obtained from the RFCs and constitute the midmonth values.

4. Methods and calibration procedure

a. Methods

The first objective of this study is to analyze the differences between MAPG, MAPX, and MAPS over a variety of basins, and to determine the dependence of relative bias on seasonality, size of the basin, and geographic location. The analysis compares datasets at the

monthly time scale as total precipitation and at the 6-h time scale using scatterplots and statistical measures [linear correlation coefficient (CORR), relative mean bias (BIAS), and normalized root-mean-square error (NRMSE)];

$$\text{BIAS} = \frac{\sum_{i=1}^{n} (\text{MAPe}_i - \text{MAPr}_i)}{n}, \quad (1)$$

$$\text{NRMSE} = \left(\sqrt{\frac{\sum_{i=1}^{n} (\text{MAPe}_i - \text{MAPr}_i)^2}{n}} \right) \Bigg/ \left(\frac{\sum_{i=1}^{n} \text{MAPr}_i}{n} \right), \quad (2)$$

where MAPe and MAPr denote the precipitation estimates under comparison (MAPe denotes either MAPX or MAPS, and MAPr denotes either MAPG or MAPX), and n is the number of 6-h dataset pairs in the analysis. The NWS utilizes a 6-h precipitation input for hydrologic forecasting in the selected study basins. Statistical measures are based on 6-h data pairs in which *either* of the datasets in the analysis reported precipitation [i.e., for the MAPX–MAPG analysis, a pair is included if either MAPX or MAPG >0 mm $(6\ \text{h})^{-1}$]. Time periods when at least one dataset is unavailable for a basin (see sections 3b–d for time periods) were excluded from the statistical measures for all dataset comparisons for all study basins. The study time period was selected to run from March 2000 through November 2003 based on data availability and was subjectively subdivided into cold (October through March) and warm (April through September) seasons in an effort to separate stratiform precipitation (large-scale organization of shallow warm clouds) from convective precipitation (small-scale patterns of thick clouds with generally cold cloud tops). A further differentiation was made to discriminate between summer (June, July, August) and winter (November, December, January).

To evaluate the utility of satellite-based precipitation estimates for flow prediction, 6-h MAPG and MAPS were used as input to the SAC-SMA model, and the resulting mean daily flows were compared with each other and with the observed flow measured at U.S. Geological Society (USGS) stations. MAPX has been excluded from this analysis due to change in the processing algorithm employed by SERFC (section 3c). Simulations were performed with parameter sets obtained through 1) manual calibration by an NWS hydrologist using historical data from a rain gauge network (hereafter RFC parameters), and 2) automatic calibration via a multistep automatic calibration scheme (MACS; Hogue et al. 2000) using data from a 23-month time period. Note that the RFC parameters are operational parameters employed by the RFCs throughout the study time period. Although the SAC-SMA parameters should be considered tied to the space and time scales for which they were calibrated (Finnerty et al. 1997), comparing MAPS-simulated flow using RFC parameters and specifically calibrated parameters will provide some insight as to whether the performance of the hydrological model improves with calibration. The model calibration period was set from October 2001 to November 2003, because this is the wettest period for which continuous precipitation data were available. Model initialization was performed using the Shuffled Complex Evolution–University of Arizona algorithm (SCE-UA; Duan et al. 1992) to optimize the initial states [using the root-mean-square error of the log-transformed flow (hereafter called LOG) as the objective function] of the model using the RFC parameters and MAPG as input (for October and November 2001). After establishing estimates of the initial states, parameter calibration was performed (using a 3-month warm-up period) for January 2002–November 2003. The verification period was set to May 2000–April 2001 based on data availability (using a 2-month warm-up period). Model initialization for the verification period was again performed using SCE-UA in a manner similar to the calibration period. We note that the verification of the model performance over one year with only a few high flows together with short warm-up period (2 months) may yield insufficient information about the model performance, and results should therefore be viewed as preliminary. Model performance evaluations are based on visual inspection of observed and simulated hydrographs, and overall statistical measures including the percent bias (% BIAS) and the Nash–Sutcliffe efficiency index (NSE):

$$\%\ \text{BIAS} = \frac{\sum_{i=1}^{n} (\text{SIM}_i - \text{OBS}_i)}{\sum_{i=1}^{n} \text{OBS}_i} (100), \quad (3)$$

$$\text{NSE} = 1 - \left[\frac{\sum_{i=1}^{n} (\text{SIM}_i - \text{OBS}_i)^2}{\sum_{i=1}^{n} (\text{OBS}_i - \text{OBS}_{\text{mean}})^2} \right], \quad (4)$$

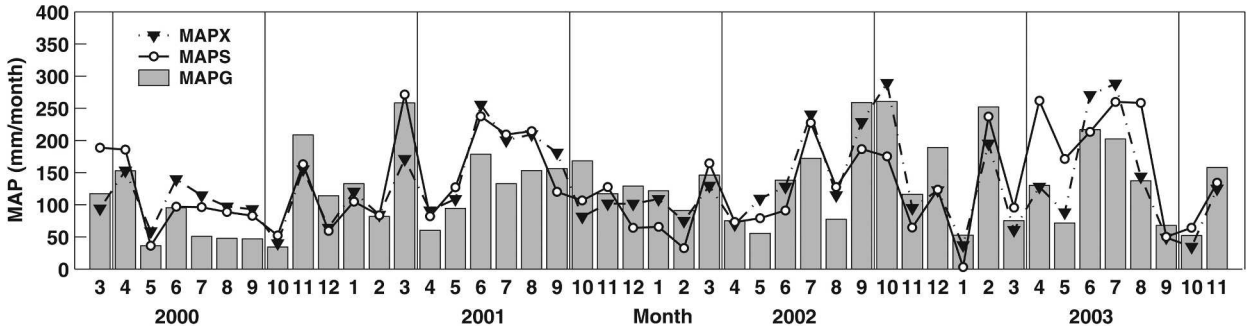

FIG. 2. Total monthly precipitation for the CLSM6 basin reported by MAPG, MAPX, and MAPS binned by month for Mar 2000–Nov 2003 (cold and warm seasons are separated by vertical lines).

where SIM is the simulated daily flow, OBS is the observed daily flow, OBS_{mean} is the mean of the observed daily flows, and n is the number of days in the analysis. NSE can vary between $-\infty$ and 1, with higher values indicating better agreement. Analysis of the timing correspondence between the five highest observed and simulated peak flows was also performed and is presented together with the hydrographs. The SJOA4 basin was excluded from flow analysis because the RFC parameters for this basin vary by season (G. Tillis, LMRFC, 2004, personal communication).

b. Calibration procedure

Calibration of the SAC-SMA model was performed using MACS (Hogue et al. 2000), which uses the SCE-UA global search algorithm and a step-by-step process to emulate the progression of steps followed by the NWS hydrologists during manual calibration. The step-by-step process is as follows: 1) Initial calibration uses the LOG objective function with 12 SAC-SMA parameters to optimize lower-zone parameters by placing a strong emphasis on fitting the low-flow portions of the hydrograph, 2) the lower-zone parameters are subsequently fixed and the remaining parameters are optimized with the daily root-mean-squared (DRMS) objective function to provide a stronger emphasis on simulating high flow events, 3) refinement of the lower-zone parameters is performed using the LOG criterion and keeping the upper-zone parameters fixed. Twelve parameters of the SAC-SMA model were calibrated while the rest were set to RFC values.

5. Results

a. Intercomparison of precipitation datasets

Because of the enormous volume of results, detailed analyses will only be shown for two representative basins, CLSM6 and CLUG1 (Fig. 1). Analysis of other basins will be provided as summary statistics, and important points will be discussed as necessary. Note that MAPS has a known detection failure during 29 January through 15 February 2003. It is worth mentioning that the following comparison is aimed at analyzing the relative differences between each precipitation dataset (MAPG, MAPX, and MAPS). These relative differences are likely due to a combination of many factors including differences in precipitation sampling area for each dataset, MAP calculation procedures, and other error characteristics (see section 2) inherent to the individual precipitation dataset.

Comparison of the monthly total precipitation amounts for the CLSM6 basin (Fig. 2) demonstrates a seasonal trend with both MAPX and MAPS overestimating (underestimating) MAPG during the warm (cold) season. For example, during the year 2001 warm season, MAPG reported 775.5 mm of precipitation whereas MAPX and MAPS reported 1046.1 and 990.1 mm of precipitation respectively, resulting in 34.9% and 27.7% more precipitation than MAPG. However, during the year 2001/02 cold season, MAPG reported 773.4 mm of precipitation whereas MAPX and MAPS reported 598.0 and 560.3 mm, respectively (22.7% and 27.5% less than MAPG). This general trend was observed throughout the study time period within the CLSM6 basin at varying degrees. In PLAM6, DARL1, and SJOA4 basins, this general seasonal trend was evident for some periods but not for others. These trends will be discussed later, together with the summary statistics.

In the CLUG1 basin (Fig. 3), MAPS and MAPG monthly totals are in good agreement throughout the time period, without any evidence of seasonal bias. MAPX also shows good agreement with MAPG during the cold season with only a slight underestimation. However, MAPX significantly overestimates MAPG and MAPS during the 2000 and 2002 warm seasons. For example, during the 2002 warm season, MAPG re-

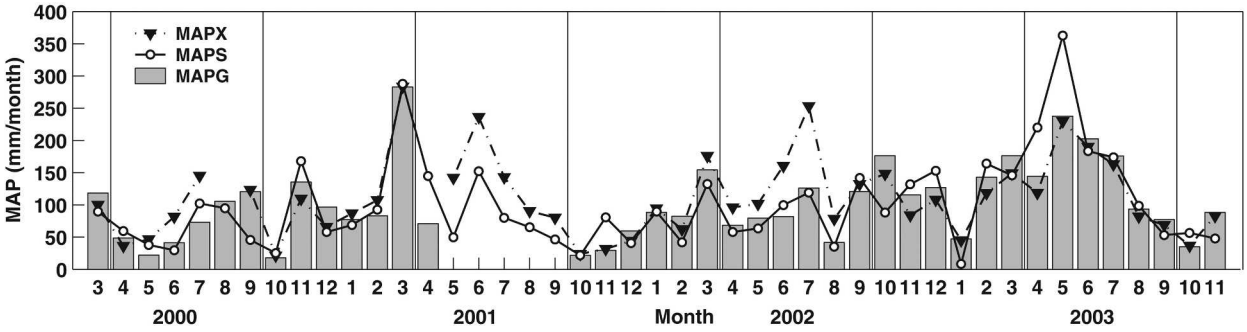

FIG. 3. Same as in Fig. 2, but for the CLUG1 basin.

ported 518.0 mm of precipitation whereas MAPX and MAPS reported 821.9 and 517.0 mm, corresponding to 58.7% overestimation and −0.2% underestimation, indicating that MAPS more closely follows MAPG monthly totals than MAPX. MAPX is in good agreement with MAPG, with a slight underestimation starting from September 2002 through the end of the study time period. Examination of the CORR statistic for the 6-h MAPG–MAPX pairs binned by month (not shown) also reveals improved correlations during this time period. This change in MAPX behavior coincides with the approximate time that the SERFC changed the multisensor processing algorithm from stage III to MPE (section 3c). The April–May 2003 period is marked by dramatically high monthly precipitation reported by MAPS, resulting from a high number of false detections. Overall, the same trend between MAPG, MAPX, and MAPS observed in CLUG1 was also evident in other Georgia basins (REDG1 and AYSG1). Progressing to 6-h time scales will allow greater insight into the results obtained from the monthly analysis.

Scatterplots in Figs. 4 and 5 result from aggregation of all available 6-h datasets for the winter and summer for the CLSM6 and CLUG1 basins, respectively. Figure 4 illustrates the same trend obtained from the monthly comparison at the 6-h time scale for the CLSM6 basin. MAPG is overestimated by MAPS [0.62 mm $(6\ \text{h})^{-1}$ BIAS] and MAPX [0.85 mm $(6\ \text{h})^{-1}$ BIAS] during summer (Figs. 4a,c) and underestimated by MAPS [−0.94 mm $(6\ \text{h})^{-1}$ BIAS] and MAPX [−1.09 mm $(6\ \text{h})^{-1}$ BIAS] during winter (Figs. 4d,f). Comparison of MAPX–MAPG, both in the summer and winter, results in better statistics than the MAPS–MAPG comparison, as indicated by the higher (lower) CORR (NRMSE). This is expected since the radar/gauge multisensor product is already corrected with the rain gauges. MAPX shows better agreement with MAPG during winter (CORR = 0.92) as opposed to summer (CORR = 0.75) (Figs. 4c,f). This may be due to possible rain gauge catch deficiency during local, short-duration summer convective storms. Smith et al. (1996) reported that even very high density rain gauge networks are unable to represent the high-rainfall-rate regions of the storm systems. Also, the procedure for disaggregating the daily rain gauge values into 6-h values employed by the RFCs may not be representative for the timing of the convective summer storms (Stellman et al. 2001). For the summer season, the comparison of MAPS–MAPG and MAPS–MAPX (Figs. 4a,b) reveals that MAPS and MAPX provide similar magnitudes for some of the high-precipitation events. The same characteristics were also observed in daily scatterplots (not shown). This behavior may be an aggregate effect of the rain gauge catch deficiency explained above and a similar behavior of MAPX and MAPS during convective storms.

In the CLUG1 basin (Fig. 5), a seasonal trend is not evident between MAPS and MAPG. Figures 5c and 5f show a general trend with MAPX overestimating MAPG during the summer [0.58 mm $(6\ \text{h})^{-1}$ BIAS] and underestimating MAPG during the winter [−0.33 mm $(6\ \text{h})^{-1}$ BIAS]. Significantly high total monthly MAPX estimates during summer (Fig. 3) can be explained by consistent overestimation of MAPG and MAPS by MAPX, which is evident in the scatterplots (Figs. 5b,c). MAPS, highly scattered around MAPG (Fig. 5a), shows reduced bias in monthly totals. Clearly, MAPX and MAPG are in better agreement during the winter than during the summer (CORR = 0.85 and 0.76, respectively) (Figs. 5c,f). In the summer, the MAPS–MAPX comparison results in higher CORR (0.63) than the MAPS–MAPG comparison (CORR = 0.52), indicating better agreement between MAPX and MAPS. It should also be noted that the Georgia basins receive much less precipitation during the analysis time period when compared to other study basins (see scatterplots) and that they contain fewer hourly rain gauges than other study basins, where almost 30% of the 6-h precipitation estimates were obtained by uniformly distributing daily estimates. Also, the Georgia basins are

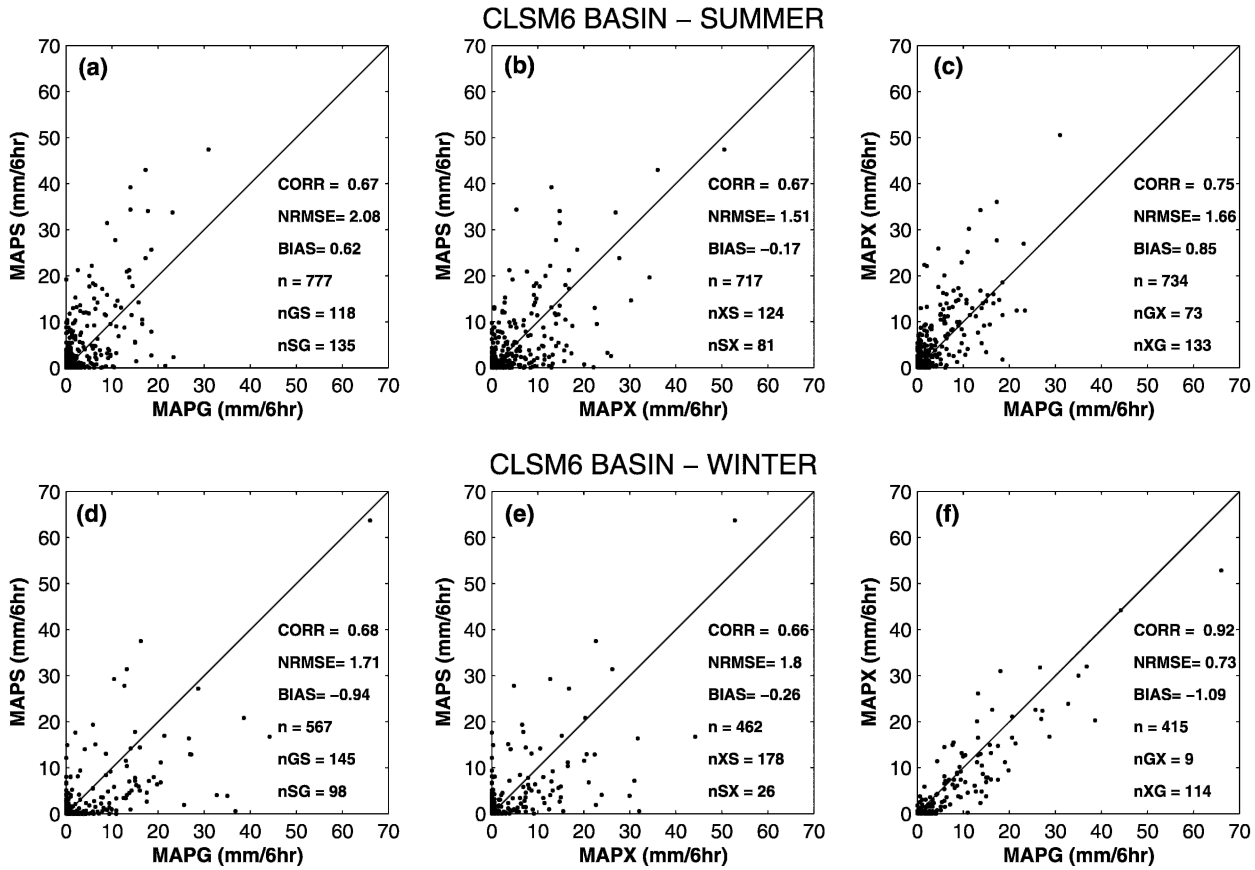

FIG. 4. Intercomparison of 6-h precipitation (mm) from MAPG, MAPX, and MAPS for the CLSM6 basin for (a), (b), (c) summer (Jun–Jul–Aug) and (d), (e), (f) winter (Nov–Dec–Jan). Here, nGS = number of data pairs where the first term estimate shows no precipitation while the second term estimate shows precipitation [i.e., rain gauge = 0 mm $(6\ \text{h})^{-1}$ and PERSIANN > 0 mm $(6\ \text{h})^{-1}$].

larger then the other study sites, and thus more satellite precipitation estimation grids are used for areal averaging, likely smoothing out the localized high precipitation rates. In the CLUG1 basin, the highest rainfall rates occur in April–May 2003. During this time period MAPS overestimates both MAPG and MAPX (Fig. 3).

To summarize the general trends between the precipitation datasets, statistical measures are presented for each study basin for summer and winter (Fig. 6). Note that basins are listed from left to right in order of increasing area and that the last three basins are located in Georgia (REDG1, AYSG1, and CLUG1). There are general trends between the datasets among the study basins. Starting with the MAPX–MAPG comparison (Figs. 6a–c), the CORR (NRMSE) statistic is higher (lower) during winter than summer for all study basins. Possible reasons were explained earlier in the discussion of Figs. 4 and 5. The SJOA4 basin has the highest (lowest) CORR (NRMSE) statistic between MAPX–MAPG. The SJOA4 basin, located within elevated terrain in Arkansas, receives precipitation in terms of short-term rapid outbreaks. The Automated Local Evaluation in Real Time (ALERT) network of the NWS established within the basin enables a large number of hourly rain gauges, thus improving the bias correction of the radar estimate. The REDG1 basin statistics result in the lowest (highest) CORR (NRMSE), especially during the summer season. Daily rainfall comparison shows a similar behavior (not given). A possible reason is the small number of rain gauges within the REDG1 basin. MAPX overestimates MAPG for every study basin (Fig. 6b) during the summer (indicated by positive bias). However, during the winter, MAPX underestimates MAPG in five out of seven basins. In the SJOA4 and DARL1 basins, MAPX shows a general trend of overestimating MAPG throughout the study time period, but this is more pronounced during the summer season. Note that these are the aggregate statistics. There were changes in the agreement between the MAPX and MAPG throughout the study time period (cf. agreement between the MAPX and MAPG for summer 2002 and 2003 in

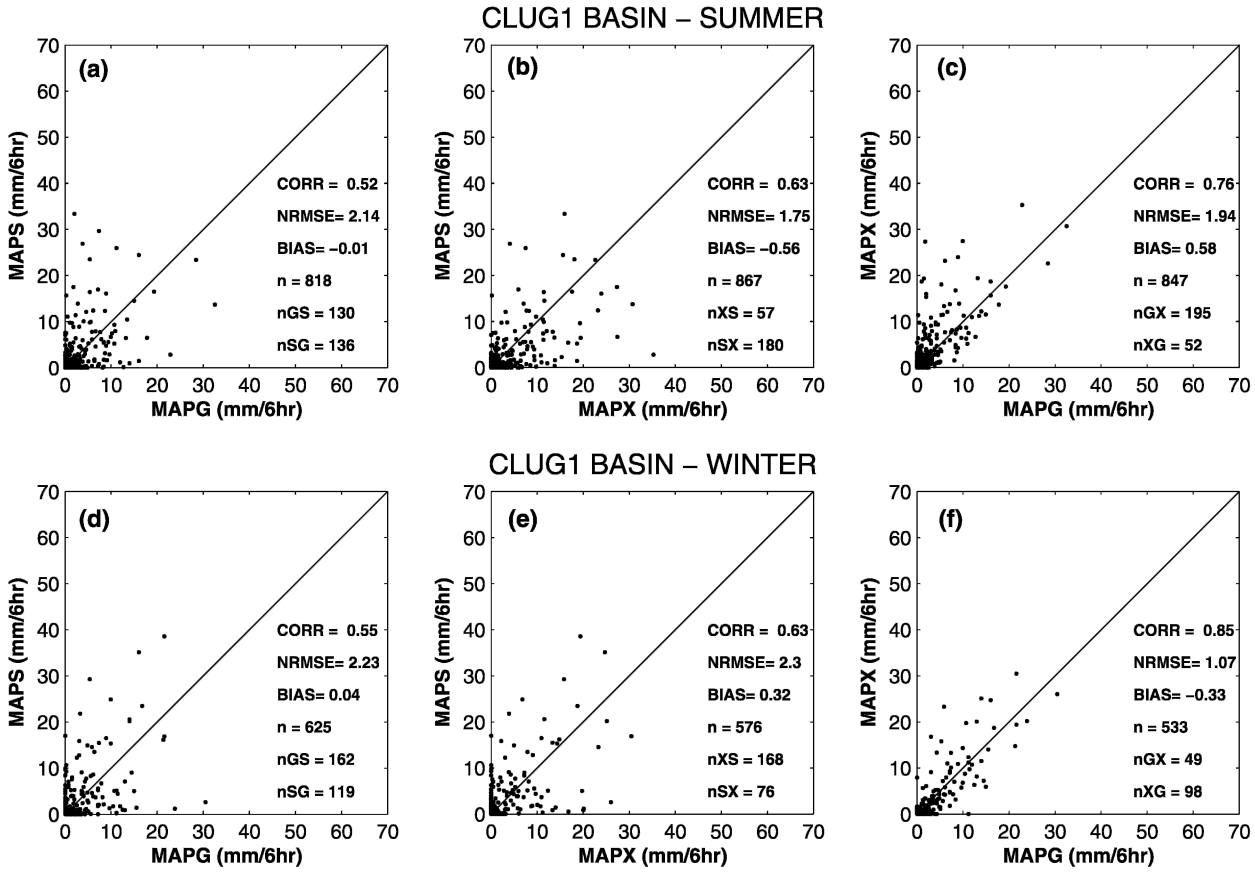

FIG. 5. Same as in Fig. 4, but for the CLUG1 basin.

Fig. 3). General CORR, BIAS, and NRMSE statistical trends for the MAPS–MAPG comparisons (Figs. 6d–f) over PLAM6, DARL1, CLSM6, and SJOA4 basins are similar to the MAPX–MAPG comparisons, but lower (higher) CORR (NRMSE) statistics indicate reduced agreement. MAPS is underestimating (overestimating) MAPG during the cold (warm) season for PLAM6, DARL1, CLSM6, and SJOA4 basins (Fig. 6e). The hyetograph comparison (not shown) indicated that under dry winter conditions, MAPS overestimates MAPG due to false precipitation detection, but given that high precipitation rates are observed by MAPG, underestimation by MAPS is evident. The MAPS–MAPG comparison (Fig. 6e) for Georgia basins (CLUG1, AYSG1, and REDG1) shows almost no bias in summer and winter seasons. A possible explanation is the fewer number of high-precipitation-rate events occurring in Georgia as opposed to other study basins. As an example, the SJOA4 and REDG1 basins are similar in size (areas are 2147 and 2939 km^2, respectively), but the SJOA4 basin is located in elevated terrain in Arkansas and receives much higher rainfall rates during the summer compared to the REDG1 basin located in Georgia. Figure 6e shows that MAPS has the highest overestimation of MAPG for the SJOA4 basin during the summer while no bias is observed for the REDG1 basin. The MAPS–MAPX comparison (Figs. 6g–i) reveals that the CORR (NRMSE) statistic is higher (lower) especially for the Georgia basins when compared to the MAPS–MAPG analysis (Figs. 6d–f). A possible explanation is that MAPS shows better agreement in timing of precipitation with MAPX than MAPG, possibly due to the smaller number of 1–6-h rain gauges.

There are several possible reasons for the observed seasonal differences between the precipitation datasets. First, rain gauges tend to underestimate local, short-duration summer convective precipitation, while providing better estimates of the larger-scale, longer-duration liquid precipitation events during the winter. However, IR-based satellite estimates tend to overestimate both area and magnitude of summer convective precipitation (Scofield and Kuligowski 2003; Rozumalski 2000; Petty and Krajewski 1996; Xie and Arkin 1995), which usually occupies only a small fraction of cold cloud area detected by the sensor. Further, IR-based techniques may produce misidentification be-

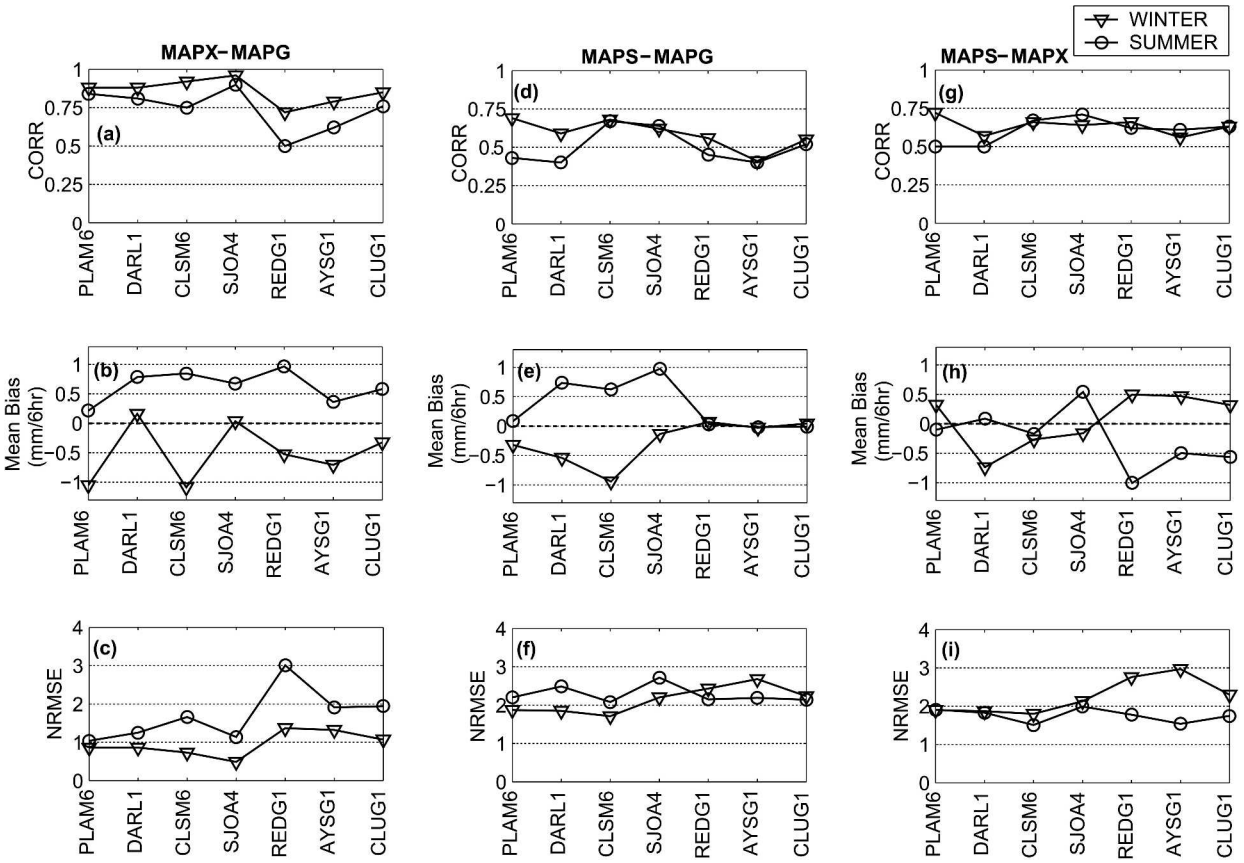

FIG. 6. Statistics of 6-h precipitation for (a), (b), (c) MAPX–MAPG; (d), (e), (f) MAPS–MAPG; and (g), (h), (i) MAPS–MAPX dataset pairs for summer and winter.

cause some cold clouds, such as cirrus, may not generate any rainfall (Kidd 2001). Underestimation by MAPS during cold seasons is likely because stratiform precipitation characterized by warm cloud tops is unlikely to give rise to a signal that can be detected by any passive (microwave or infrared) technique (Scofield and Kuligowski 2003; Petty and Krajewski 1996). Special Sensor Microwave Imager (SSM/I) (DMSP satellite) precipitation rates may also result in underestimation because it is sensitive to scattering by frozen precipitation particles in the upper portions of the cold clouds, but not all rain-bearing clouds contain such ice particles (Petty and Krajewski 1996). In basins where a fewer number of satellite precipitation estimation grids are used, these biases are expected to become more pronounced.

Finally, underestimation by MAPX in the winter months is due mostly to shallow stratiform precipitation systems in which the radar beam overshoots the upper level of rainfall, especially at far range (Fulton et al. 1998; Stellman et al. 2001; Grassotti et al. 2003). Overestimation by MAPX during summer is likely due to the presence of mixed precipitation (i.e., hail, graupel, ice falling through melting layers, etc.), which produces unreasonably high rain rates within a *Z–R* relationship (Fulton et al. 1998; Grassotti et al. 2003). The seasonal bias observed in the stage III multisensor product during various periods over several study basins was also observed by Grassotti et al. (2003) in a radar-only product (WSI). This similarity may indicate the lack of a sufficient number of rain gauges for radar bias correction and inadequate quality control procedures for the stage III multisensor product.

b. Evaluation of flow predictions

This subsection analyzes the utility of satellite precipitation estimates for flow prediction. The MAPG- and MAPS-driven SAC-SMA model-simulated flows were generated using both the RFC parameters (RFC-MAPG, RFC-MAPS) and calibrated parameters (CAL-MAPG, CAL-MAPS) and evaluated in terms of overall statistical measures, (% BIAS) and NSE (Fig. 7), and visual examination of hydrographs, residuals, and peak timing (Figs. 8–11). To better visualize the

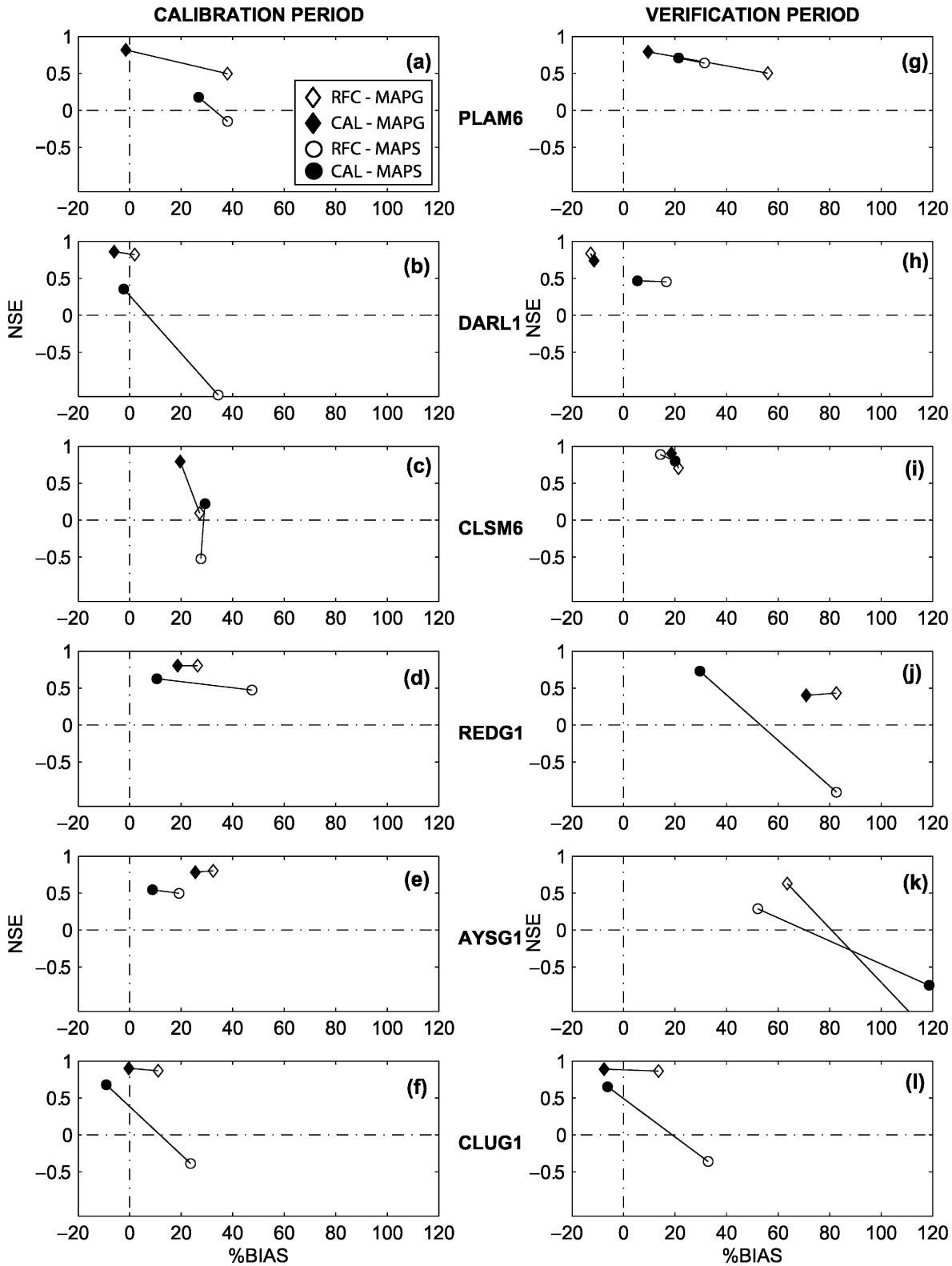

FIG. 7. Evaluation of model performance over study basins for the (a)–(f) calibration and (g)–(l) verification period. (Lines denote the improvement in performance when model parameters are changed from RFC to CAL.)

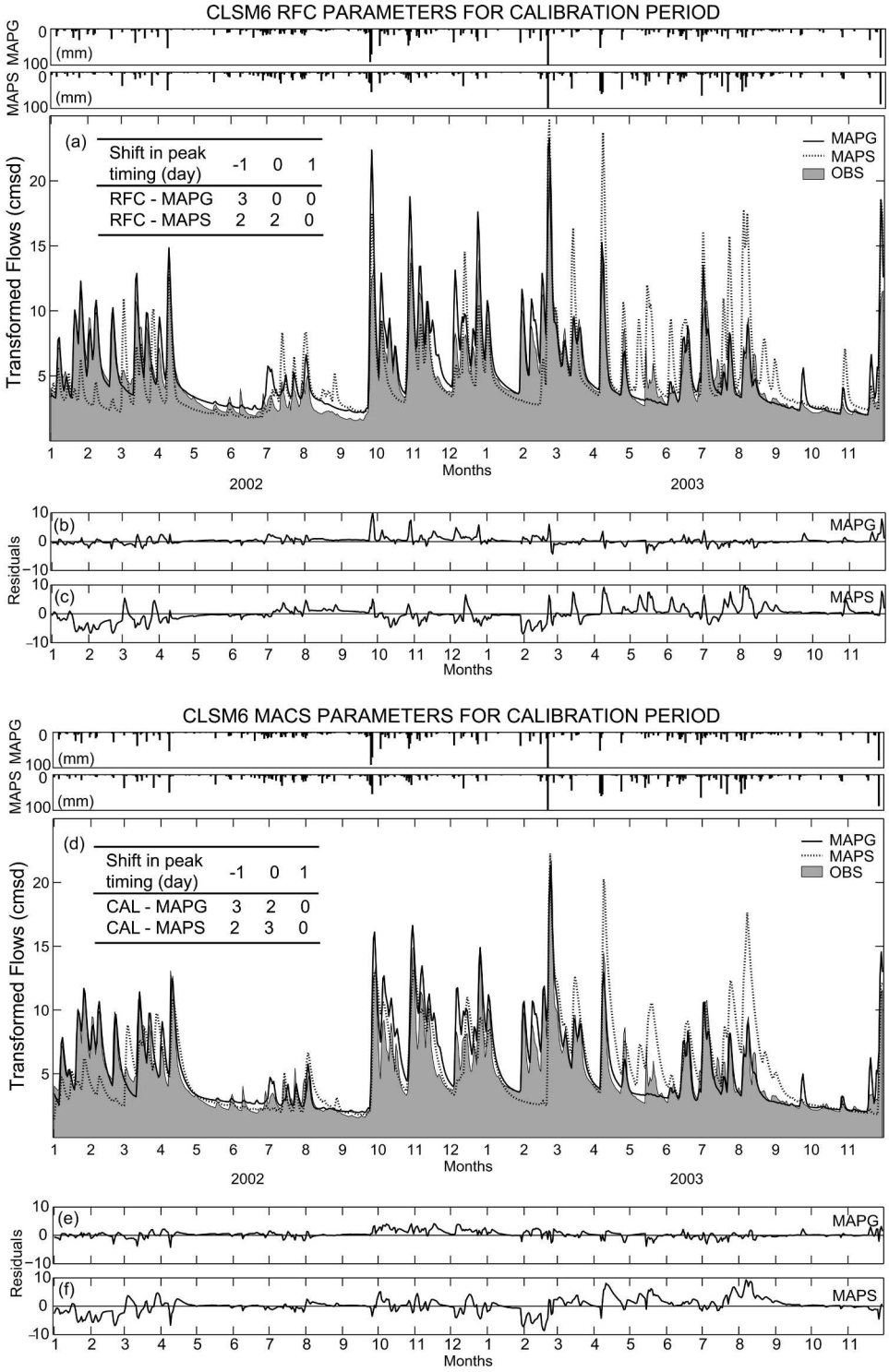

FIG. 8. CLSM6 basin calibration period. RFC parameters simulation (a) hydrographs, (b) RFC-MAPG residuals, and (c) RFC-MAPS residuals. MACS parameters simulation (d) hydrographs, (e) CAL-MAPG residuals, and (f) CAL-MAPS residuals. The number of peak events predicted within ±1 day time window around the five highest observed peak flows is also provided with the hydrographs.

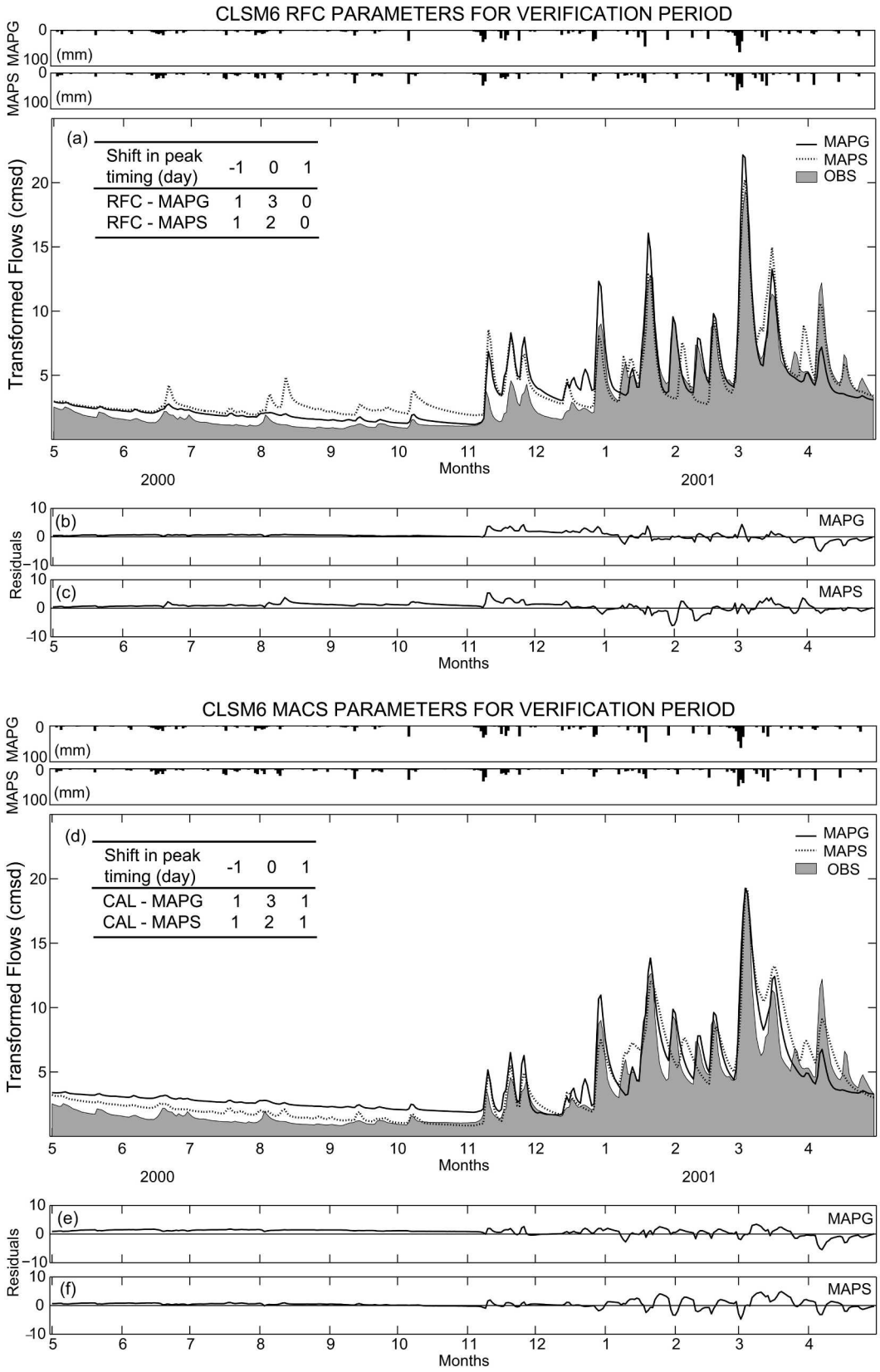

FIG. 9. Same as in Fig. 8, but for the verification period.

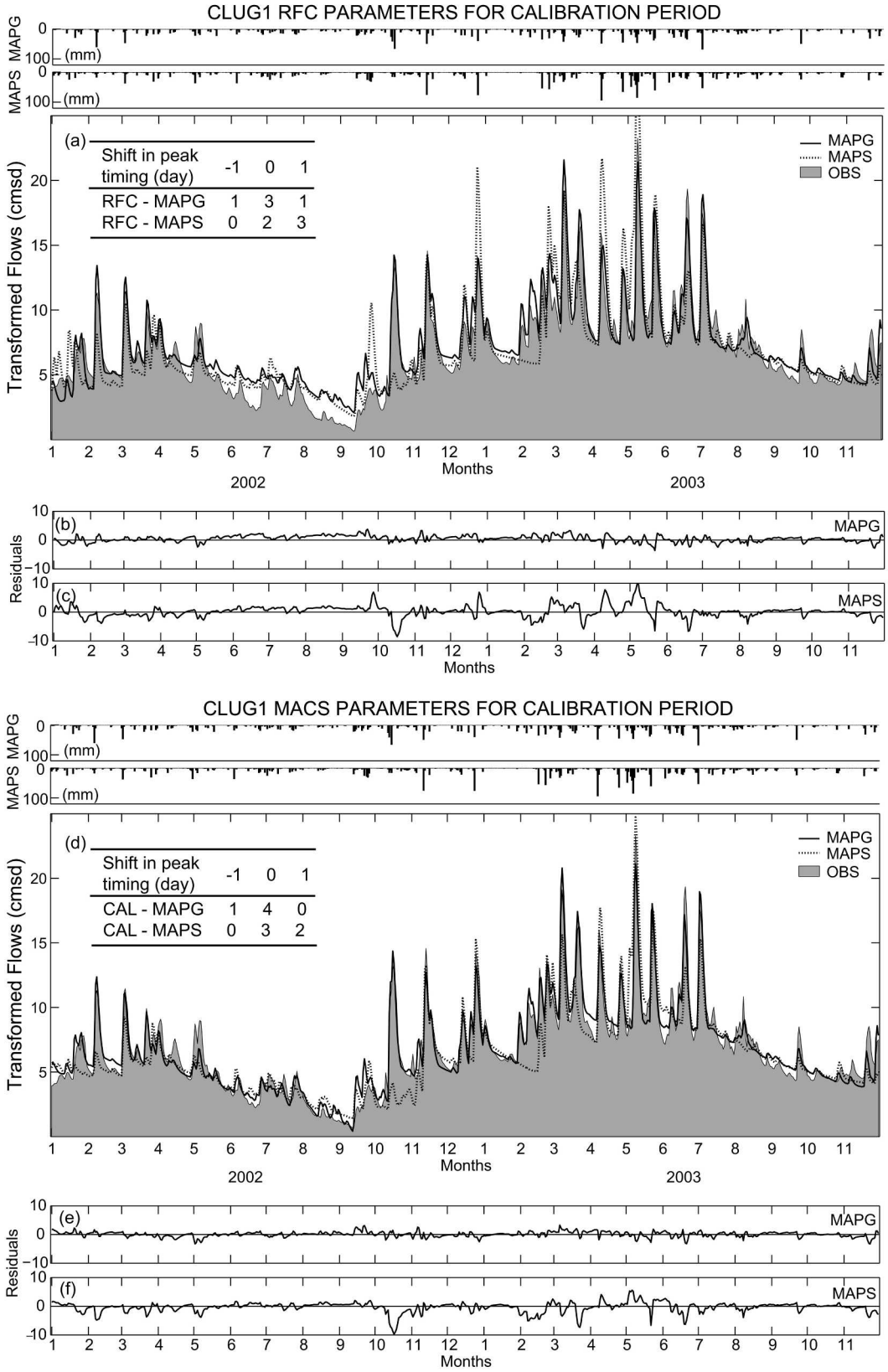

FIG. 10. Same as in Fig. 8, but for CLUG1.

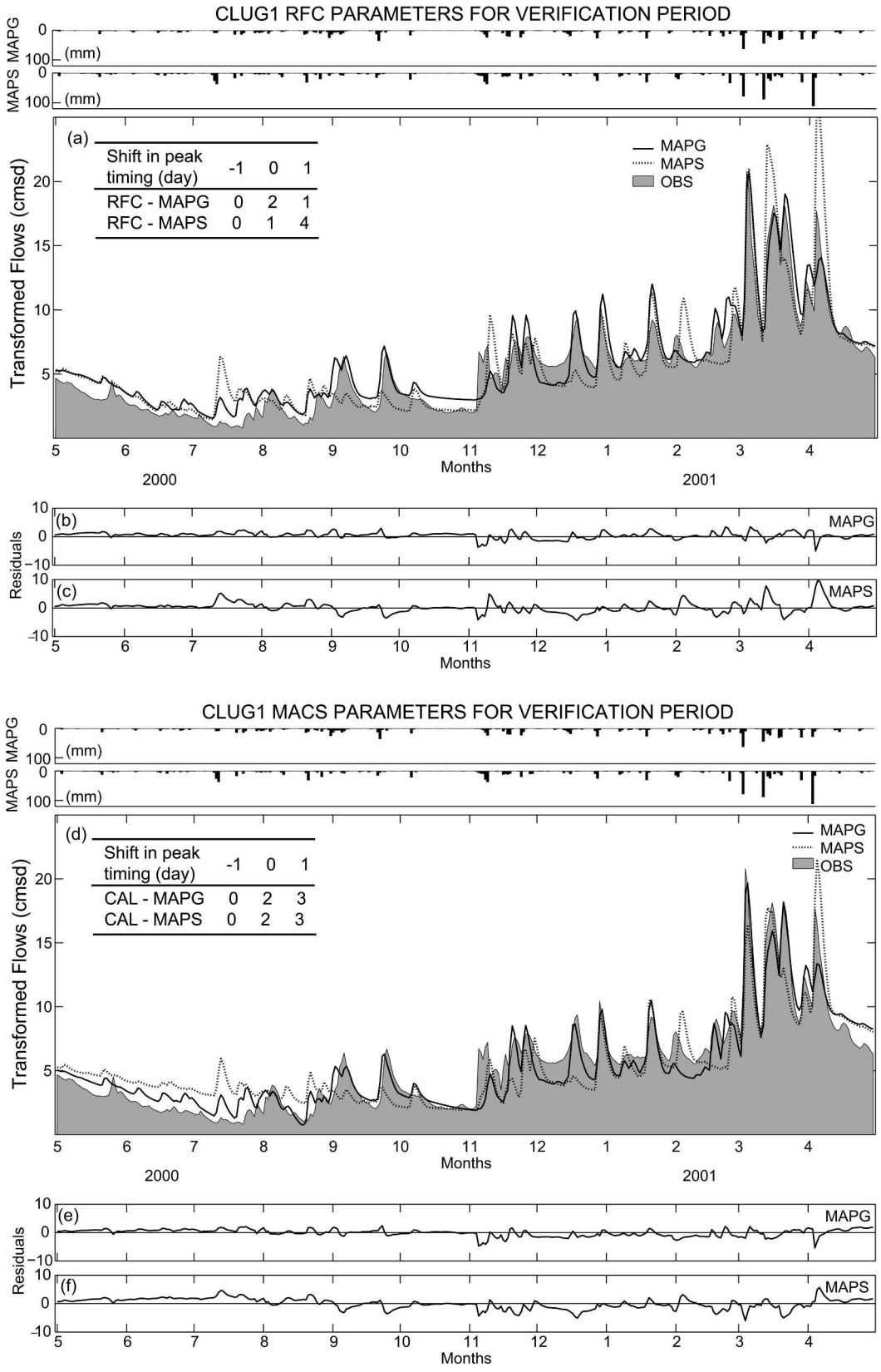

FIG. 11. Same as in Fig. 8, but for the CLUG1 verification period.

flow performance over the full range of flows, hydrographs are plotted in the transformed space

$$Q_{\text{transformed}} = \frac{(Q+1)^{\lambda} - 1}{\lambda}, \quad (5)$$

where Q is the flow and λ is a transformation parameter, which is set to 0.3 (after evaluating the visual effect provided by a full range of λ values).

1) RFC PARAMETERS

The overall statistics (Fig. 7) show that the RFC-MAPG simulation generally resulted in reasonable NSE statistics with a minimum for the PLAM6 basin (NSE = 0.5). An exception is the CLSM6 basin where poor performance (NSE = 0.1) is observed, possibly due to the large overestimation of the observed peaks during October–December 2002 and poor matching of the peak timing (Fig. 8a). Overall, a large positive % BIAS results from the RFC-MAPG simulations (reaching up to 38% for the PLAM6 basin during the calibration period). Verification period statistics also show a large positive % BIAS for RFC-MAPG (especially in the Georgia basins), most likely due to the prevailing dry conditions. RFC-MAPS, on the other hand, resulted in negative NSE statistics for CLSM6, DARL1, PLAM6, and CLUG1 basins during the calibration period, indicating simulation predictions are not as good as simply using the observed mean as a predictor. In the CLSM6 basin, the RFC-MAPS (Figs. 8a,c) significantly overestimated peak flows during spring–summer 2003. A major overestimation is evident around 9 April 2003 with an observed peak flow of 266 cm. During this event, MAPS reported 197 mm of rainfall in three days with a peak flow of 1073 cm (300% BIAS) on the same day, while MAPG reported 83.5 mm and a peak flow of 307 cm (15% BIAS) one day earlier than observed. Overestimation of peak flows during spring and summer are also evident in the PLAM6 and DARL1 basin RFC-MAPS simulations (not shown). In the CLSM6 basin, RFC-MAPS (Figs. 8a,c) resulted in a general underestimation of flows during the winter, with the exception of several overestimated peak flows (see mid-December 2002). Throughout the calibration period RFC-MAPS shows both false (mid-May 2003) and missed (mid-October 2002) peak flows, which are properly depicted by the MAPG.

In the CLUG1 basin, RFC-MAPG results in good overall performance (Fig. 7f) (0.87 NSE; 11% BIAS) and a good match between the observed and simulated hydrographs (Figs. 10a,b). RFC-MAPS, on the other hand, has particular difficulty with both over- and underestimations during winter 2002 and spring 2003. A major overestimation of peak flow by RFC-MAPS is evident on 9 May 2003 with an observed flow of 1014 cm. During this event, MAPS reported 183.7 mm of rainfall in 4 days with a peak flow of 2235 cm (120% BIAS) while MAPG reported 97 mm and a peak flow of 798 cm (21% BIAS). Another interesting event occurs in early October 2002, when RFC-MAPS missed a peak flow, which is properly diagnosed by RFC-MAPG.

During the verification period (Figs. 7g–l), the RFC-MAPS for the CLSM6 and PLAM6 basins show better model performance than the RFC-MAPG as indicated by higher (lower) NSE (% BIAS). This situation can be explained using Fig. 9a, in which RFC-MAPG simulations overestimated the high-flow events. This result may be due to error in the MAPG estimates, but also to error in the evapotranspiration estimates since overestimation was also seen in winter/early fall 2002 (Fig. 8a).

2) CALIBRATED PARAMETERS

The previous subsection illustrated that model performance significantly reduces when utilizing satellite-based precipitation estimates with RFC parameters. This subsection introduces model calibration efforts to analyze whether an improvement in the performance of a model driven by MAPS and MAPG can be achieved based on calibration using a relatively short period of data (23 months).

The overall statistics (Figs. 7a–f) show comparatively better model performance with calibrated parameters compared to the RFC parameters for both MAPG and MAPS simulations. In the CLSM6 basin, a significant improvement in the calibration period is observed for CAL-MAPG when compared to RFC-MAPG (NSE changed from 0.1 to 0.8), followed however by only minor improvement for the verification period. Analysis of the hydrographs for the calibration period (Figs. 8a–e) shows that the improvement in model performance is mainly due to the better estimation of flows during October–December 2002 and better matching in timing of the peak flows. Another significant improvement with CAL-MAPG, both in terms of NSE and % BIAS, is obtained for the PLAM6 basin, which is also followed by significant improvement in the verification period. For the DARL1, CLUG1, AYSG1, and REDG1 basins, CAL-MAPG resulted in minor improvements in model performance. CAL-MAPS, on the other hand, yields performance improvements for every basin during the calibration period, but the CLSM6 and PLAM6 basins still suffer from poor performance. Improvement in model performance for the CLSM6 basin, when using CAL-MAPS, is mainly

due to a decrease in overestimation of peak flows and also a better simulation of peak timing (Figs. 8a,d). While parameter adjustments compensated for some of the error in the MAPS input, calibration also resulted in increased errors during the recessions and low flows (see April, May, and August 2003). In the CLUG1 basin (Figs. 7f, 10), model performance improvement is mainly due to the elimination of false high flows by CAL-MAPS compared to RFC-MAPS. For example, the highest observed flow event (1014 cm) occurring on 9 May 2003 was reduced from 2350 cm (120% BIAS) for RFC-MAPS to 1200 cm (18% BIAS) for CAL-MAPS. In the CLUG1 basin, the verification performance for CAL-MAPS (0.65 NSE and −6.5% BIAS) is in line with the calibration performance and slightly poorer than the CAL-MAPG performance during verification (0.89 NSE and −7.5% BIAS). In the CLUG1 basin verification period (Fig. 11d), both CAL-MAPS and CAL-MAPG had difficulty in predicting peak flows during March–April 2001, but CAL-MAPG better represented the lower peak flows (see September and December 2000).

In the AYSG1 basin (Figs. 7e,k), although the calibrated parameters resulted in slightly improved performance over the RFC parameters during the calibration period, they failed to capture the observed flows during the verification period (NSE ~ -1 and BIAS $>100\%$). The REDG1 basin (Figs. 7d,j) shows improved model performance due to model calibration, not only during the calibration period but also during the verification period. In the verification period, CAL-MAPS resulted in even better performance than CAL-MAPG. Analysis of the hydrographs (not shown) indicates that both CAL-MAPG and CAL-MAPS tend to strongly overestimate the dry conditions prevailing during May–September 2000 in the REDG1 basin, but it also revealed that the CAL-MAPG simulations overestimate the relatively high flow conditions during winter/spring 2001. The SERFC has also reported particular difficulty in calibration of the AYSG1 and REDG1 basins (J. Bradberry, SERFC, 2004, personal communication).

As an overall summary, calibration of the SAC-SMA model with satellite precipitation estimates has improved the model performance in both the calibration and verification periods when compared to the model simulations with RFC parameters. But MAPS-driven model performances were still poor for the PLAM6, DARL1, and CLSM6 basins, which are smaller in size and produced high biases between MAPG and MAPS. Poor model performance even for the calibration period is an indication of an inability of the model and the calibration procedure to filter out the variation and error in MAPS. Better performances obtained for the CLUG1 (slightly poorer than rain gauge calibration) and REDG1 (better than rain gauge calibration during verification period) basins are probably due to the large size of these basins and a smaller bias between MAPG and MAPS. Again, note that short calibration and verification time periods may also have an effect on these results.

6. Conclusions and recommendations

The objective of this study was to evaluate the utility of satellite-based precipitation estimates for hydrologic forecasting, as they may provide the only source of precipitation for areas where ground-based networks are unavailable. The results of our precipitation intercomparison study performed at seven basins within the southeastern United States show that agreements between the precipitation datasets vary from basin to basin and also temporally within the basins. General conclusions from the three-way intercomparison of the datasets are provided below. Please note that these are *relative* comparisons only.

1) MAPS tends to provide larger estimates than MAPG during the warm season and smaller estimates than MAPG during the cold season for the basins located in Mississippi, Louisiana, and Arkansas. This warm-season trend is most pronounced for the Arkansas basin. In the Georgia basins, a seasonal trend was not evident between the MAPG and MAPS, and fairly good agreements in terms of monthly totals and overall bias were observed.
2) MAPX tends to provide slightly larger estimates than MAPG for the basins in Louisiana and Arkansas regardless of the season; however, this tendency is more pronounced during the warm season. In the Mississippi basins, MAPX tends to provide larger estimates than MAPG during the warm season and smaller estimates during the cold season. In the Georgia basins, the MAPX–MAPG comparison shows large variation. MAPX provides considerably larger estimates than MAPG during the warm season in the earlier time periods, but better agreement (with slightly smaller estimates) in the later time period. This change is probably due to the change in the radar-processing algorithm (from stage III to MPE) implemented by the SERFC. At the 6-h time scale, the correlation between MAPX and MAPG is higher for winter stratiform precipitation than summer convective precipitation. This difference is

more pronounced for the two basins in Georgia, in which a fewer hourly rain gauges are present.

3) The MAPS–MAPX comparison shows smaller bias than the MAPS–MAPG comparison at some time periods but larger bias in other periods. This is mainly due to a similar MAPX and MAPS response to stratiform and convective precipitation patterns in some basins (although for different reasons), but is complicated by calibration differences between radars, availability of hourly rain gauges for radar bias correction, degree of radar quality control, and geographic location.

Results from the evaluation of the hydrological model performance show that, when using satellite-based precipitation estimates, even short time periods of model calibration can considerably improve model performance compared to manually calibrated parameters using historical rain gauge data (RFC parameters). Of course, the degree of improvement may vary with basin size and location. These results can be summarized as follows.

1) When MAPS is used to drive the model with RFC parameters, major deterioration in model performance is observed when compared with the MAPG-driven model. We observe positive streamflow prediction bias in all study basins, and negative Nash–Sutcliffe efficiencies in four out of six basins. Calibration improves model performance in all basins as expected, but the results are not satisfactory for basins in Mississippi and Louisiana (even for the calibration period). The better calibration performance obtained with MAPG (indicated by NSE and % BIAS statistics) suggests problems with the MAPS product. The poor MAPS results may be attributed to the large differences between MAPS and MAPG over these basins, which may be partly due to the fact that these basins are smaller in size and therefore there is less smoothing of the precipitation variation and error. For the two Georgia basins, model calibration using MAPS resulted in significantly improved model performance (for both calibration and verification periods)—these are also the basins showing better agreement between MAPS and MAPG. Note, however, that for all the studies conducted here the calibration and verification periods used were for relatively short and dry conditions—those results should therefore be only viewed as preliminary.
2) Changes/improvements in the radar/gauge multisensor precipitation-processing algorithms (such as transition from stage III to MPE) affect the behavioral characteristics of this dataset. These behavioral changes must be properly taken into account when such data are used for model calibration and/or evaluation in future studies.

As a future extension of this analysis, different hydroclimatic regions (e.g., semiarid) over different parts of the world will be selected with varying basin sizes and rain gauge network densities to further test the possible benefits of using satellite-based precipitation estimates for flow prediction. The availability of these estimates at finer spatial scales will improve their applicability to basin-scale hydrologic applications, especially when using distributed models. Also, inclusion of error estimates associated with satellite-based precipitation products will enable hydrologists to define confidence limits on the hydrologic predictions. As a natural extension of this work for ungauged basin studies, satellite-based precipitation estimates will be used together with model parameters derived from basin characteristics, rather than calibrated through observed streamflow.

We have demonstrated that although satellite-based precipitation estimates contain errors that can affect flow predictions, there is clear potential for use of these products in hydrologic forecasting and water management. This potential is expected to increase with the launch of new satellites. The neural network structure of the PERSIANN system can easily be adapted to incorporate new information as it becomes available.

Acknowledgments. Support for this work was provided by NASA Jet Propulsion Laboratory (Grant 1236728), the Center for Sustainability of semi-Arid Hydrology and Riparian Areas (SAHRA) (EAR-9876800), the Hydrology Laboratory of the National Weather Service (Grants NA87WHO582 and NA07WH0144), NASA-EOS (Grant NA56GPO185), TRMM (Grant NAG5-7716), and the International Centre for Scientific Culture—World Laboratory. We thank the personnel of Lower Mississippi and Southeast River Forecast Centers for their help and guidance. We would also like to thank David R. Legates and anonymous reviewers for their constructive comments.

REFERENCES

Adler, R. F., G. J. Huffman, D. T. Bolvin, S. Curtis, and E. J. Nelkin, 2000: Tropical rainfall distributions determined using TRMM combined with other satellite and rain gauge information. *J. Appl. Meteor.,* **39,** 2007–2023.

——, C. Kidd, G. Petty, M. Morrissey, and H. M. Goodman, 2001: Intercomparison of global precipitation products: The third

Precipitation Intercomparison Project (PIP-3). *Bull. Amer. Meteor. Soc.,* **82,** 1377–1396.

Andreassian, V., C. Perrin, C. Michel, I. Usart-Sanchez, and J. Lavabre, 2001: Impact of imperfect rainfall knowledge on the efficiency and the parameters of watershed models. *J. Hydrol.,* **250,** 206–223.

Brazil, L. E., and M. D. Hudlow, 1981: Calibration procedures used with the National Weather Service River Forecast System. *Water and Related Land Resource Systems*, Y. Y. Haimes and J. Kindler, Eds., Pergamon, 457–566.

Burnash, R. J. C., 1995: The NWS River Forecast System—Catchment modeling. *Computer Models of Watershed Hydrology,* V. P. Singh, Ed., Water Resources Publications, 311–366.

——, R. L. Ferral, and R. A. McGuire, 1973: A generalized streamflow simulation system—Conceptual modeling for digital computers. Joint Federal–State River Forecast Center Tech. Rep., Department of Water Resources, State of California and National Weather Service, 204 pp.

Duan, Q. Y., S. Sorooshian, and H. V. Gupta, 1992: Effective and efficient global optimization for conceptual rainfall-runoff models. *Water Resour. Res.,* **28,** 1015–1031.

Ferraro, R. R., and G. F. Marks, 1995: The development of SSM/I rain-rate retrieval algorithms using ground-based radar measurements. *J. Atmos. Oceanic Technol.,* **12,** 755–770.

Finnerty, B. D., M. B. Smith, D.-J. Seo, V. Koren, and G. E. Moglen, 1997: Space–time scale sensitivity of the Sacramento model to radar-gage precipitation inputs. *J. Hydrol.,* **203,** 21–38.

Fulton, R. A., 2002: Activities to improve WSR-88D radar rainfall estimation in the National Weather Service. *Proc. Second Federal Interagency Hydrologic Modeling Conf.,* Las Vegas, NV, Subcomittee on Hydrology, Advisory Committee on Water Data, CD-ROM. [Available online at http://www.nws.noaa.gov/oh/hrl/presentations/fihm02/pdfs/qpe_hydromodelconf_web.pdf.]

——, J. P. Breidenbach, D.-J. Seo, D. A. Miller, and T. O'Bannon, 1998: The WSR-88D rainfall algorithm. *Wea. Forecasting,* **13,** 377–395.

Grassotti, C., R. N. Hoffman, E. R. Vivoni, and D. Entekhabi, 2003: Multiple-timescale intercomparison of two radar products and rain gauge observations over the Arkansas–Red River basin. *Wea. Forecasting,* **18,** 1207–1229.

Grimes, D. I. F., and M. Diop, 2003: Satellite-based rainfall estimation for river flow forecasting in Africa. I: Rainfall estimates and hydrological forecasts. *Hydrol. Sci. J.,* **48,** 567–584.

Groisman, P. Y., and D. R. Legates, 1994: The accuracy of United States precipitation data. *Bull. Amer. Meteor. Soc.,* **75,** 215–227.

Gupta, H. V., K. J. Beven, and T. Wagener, 2005: Model calibration and uncertainty estimation. *Encyclopedia of Hydrological Sciences*, M. G. Anderson, Ed., John Wiley & Sons, in press.

Hogue, T. S., S. Sorooshian, H. V. Gupta, A. Holz, and D. Braatz, 2000: A multistep automatic calibration scheme for river forecasting models. *J. Hydrometeor.,* **1,** 524–542.

Hsu, K., X. Gao, S. Sorooshian, and H. V. Gupta, 1997: Precipitation estimation from remotely sensed information using artificial neural networks. *J. Appl. Meteor.,* **36,** 1176–1190.

——, H. V. Gupta, X. Gao, and S. Sorooshian, 1999: Estimation of physical variables from multiple channel remotely sensed imagery using a neural network: Application to rainfall estimation. *Water Resour. Res.,* **35,** 1605–1618.

——, ——, ——, ——, and B. Imam, 2002: Self-organizing linear output map (SOLO): An artificial neural network suitable for hydrologic modeling and analysis. *Water Resour. Res.,* **38,** 1302, doi:10.1029/2001WR000795.

Huffman, G. J., R. F. Adler, M. Morrissey, D. T. Bolvin, S. Curtis, R. Joyce, B. McGavock, and J. Susskind, 2001: Global precipitation at one-degree daily resolution from multisatellite observations. *J. Hydrometeor.,* **2,** 36–50.

Johnson, D., M. Smith, V. Koren, and B. Finnerty, 1999: Comparing mean areal precipitation estimates from NEXRAD and rain gauge networks. *J. Hydrol. Eng.,* **2,** 117–124.

Kidd, C., 2001: Satellite rainfall climatology: A review. *Int. J. Climatol.,* **21,** 1041–1066.

Koren, V. I., B. D. Finnerty, J. C. Schaake, M. B. Smith, D.-J. Seo, and Q. Y. Duan, 1999: Scale dependencies of hydrologic models to spatial variability of precipitation. *J. Hydrol.,* **217,** 285–302.

Krajewski, W. F., G. J. Ciach, J. R. McCollum, and C. Bacotiu, 2000: Initial validation of the Global Precipitation Climatology Project monthly rainfall over the United States. *J. Appl. Meteor.,* **39,** 1071–1086.

Kuligowski, R. J., 2002: A self-calibrating real-time GOES rainfall algorithm for short-term rainfall estimates. *J. Hydrometeor.,* **3,** 112–130.

Kummerow, C., W. Barnes, T. Kozu, J. Shiue, and J. Simpson, 1998: The Tropical Rainfall Measuring Mission (TRMM) sensor package. *J. Atmos. Oceanic Technol.,* **15,** 809–816.

Legates, D. R., and T. L. DeLiberty, 1993: Precipitation measurement biases in the United States. *Water Resour. Bull.,* **29,** 855–861.

McCollum, J. R., W. F. Krajewski, R. R. Ferraro, and M. B. Ba, 2002: Evaluation of biases of satellite rainfall estimation algorithms over the continental United States. *J. Appl. Meteor.,* **41,** 1065–1080.

Morin, E., W. F. Krajewski, D. C. Goodrich, X. Gao, and S. Sorooshian, 2003: Estimating rainfall intensities from weather radar data: The scale-dependency problem. *J. Hydrometeor.,* **4,** 782–797.

Petty, G., and W. F. Krajewski, 1996: Satellite estimation of precipitation over land. *Hydrol. Sci. J.,* **41,** 433–451.

Rozumalski, R. A., 2000: A quantitative assessment of the NESDIS Auto-Estimator. *Wea. Forecasting,* **15,** 397–415.

Scofield, R. A., and R. J. Kuligowski, 2003: Status and outlook of operational satellite precipitation algorithms for extreme-precipitation events. *Wea. Forecasting,* **18,** 1037–1051.

Seo, D.-J., R. A. Fulton, and J. P. Breidenbach, 1997: Interagency memorandum of understanding among the NEXRAD program, WSR-88D Operational Support Facility, and the NWS/OH Hydrologic Research Laboratory. NWS/OH Hydrologic Research Laboratory Final Report, Silver Spring, MD. [Available from NWS/OH/HRL, 1325 East–West Hwy., W/OH1, Silver Spring, MD 20910.]

Sivapalan, M., and Coauthors, 2003: IAHS decade on Predictions in Ungauged Basins (PUB), 2003–2012: Shaping an exciting future for the hydrological sciences. *Hydrol. Sci. J.,* **48,** 857–880.

Smith, J. A., D. J. Seo, M. L. Baeck, and M. D. Hudlow, 1996: An intercomparison study of NEXRAD precipitation estimates. *Water Resour. Res.,* **32,** 2035–2045.

Sorooshian, S., K. Hsu, X. Gao, H. V. Gupta, B. Imam, and D. Braithwaite, 2000: Evaluation of PERSIANN system satel-

lite-based estimates of tropical rainfall. *Bull. Amer. Meteor. Soc.,* **81,** 2035–2046.

Stellman, K. M., H. E. Fuelberg, R. Garza, and M. Mullusky, 2001: An examination of radar and rain gauge–derived mean areal precipitation over Georgia watersheds. *Wea. Forecasting,* **16,** 133–144.

Tsintikidis, D., K. P. Georgakakos, G. A. Artan, and A. A. Tsonis, 1999: A feasibility study on mean areal rainfall estimation and hydrologic response in the Blue Nile region using METEOSAT images. *J. Hydrol.,* **221,** 97–116.

Weng, F., L. Zhao, R. R. Ferraro, G. Poe, X. Li, and N. C. Grody, 2003: Advanced microwave sounding unit cloud and precipitation algorithms. *Radio Sci.,* **38,** 8068, doi:10.1029/2002RS002679.

Winchell, M., H. V. Gupta, and S. Sorooshian, 1998: On the simulation of infiltration- and saturation-excess runoff using radar-based rainfall estimates: Effects of algorithm uncertainty and pixel aggregation. *Water Resour. Res.,* **34,** 2655–2670.

Xie, P., and P. A. Arkin, 1995: An intercomparison of gauge observations and satellite estimates of monthly precipitation. *J. Appl. Meteor.,* **34,** 1143–1160.

——, and ——, 1997: Global precipitation: A 17-year monthly analysis based on gauge observations, satellite estimates, and numerical model outputs. *Bull. Amer. Meteor. Soc.,* **78,** 2539–2558.

Young, C. B., A. A. Bradley, W. F. Krajewski, A. Kruger, and M. L. Morrissey, 2000: Evaluating NEXRAD multisensor precipitation estimates for operational hydrologic forecasting. *J. Hydrometeor.,* **1,** 241–254.